J Therm Anal Calorim (2013) 112:1317–1323
DOI 10.1007/s10973-012-2713-8

A study of thermal and dielectric behavior of melaminium perchlorate monohydrate single crystals

N. Kanagathara · M. K. Marchewka · N. Sivakumar · K. Gayathri · N. G. Renganathan · S. Gunasekaran · G. Anbalagan

Received: 26 June 2012 / Accepted: 17 September 2012 / Published online: 9 October 2012

Abstract Single crystals of melaminium perchlorate monohydrate (MPM) have been grown from aqueous solution by slow solvent evaporation method at room temperature. X-ray powder diffraction analysis confirms the title crystal crystallizes in the triclinic (P-1) structure and the calculated lattice parameters are $a = 5.6275 \pm 0.0780$ Å, $b = 7.6926 \pm 0.1025$ Å, $c = 12.0878 \pm 0.2756$ Å, $\alpha = 103.89 \pm 1.01°$, $\beta = 94.61 \pm 0.92°$, $\gamma = 110.22 \pm 0.81°$, and $V = 468.95$ Å^3. The thermal decomposition behavior of MPM has been studied by means of thermogravimetric analysis at three different heating rates 5, 10, and 20 °C min^{-1}. The values of effective activation energy (E_a), pre-exponential factor (ln A) of each stage of thermal decomposition for all heating rates were calculated by model free method: Kissinger, Kim–Park, and Flynn–Wall method. A significant variation of effective activation energy (E_a) with conversion (α) indicates that the process is kinetically complex. The linear relationship between the A and E_a values was established (compensation effect). Dielectric study has also been carried out and it is found that both dielectric constant (ε') and dielectric loss (ε'') decreases with increase in frequency.

Keywords Melaminium perchlorate monohydrate (MPM) · Energy of activation · Thermal properties · Kinetics · Dielectric constant · Dielectric loss

Introduction

Melamine (2,4,6-triamino-1,3,5-triazine) is an industrial chemical mainly used in the production of melamine formaldehyde resins for surface coatings, laminates, and adhesives and in the production of flame retardants resins to improve the flame resistance [1]. The use of melamine resin in automobile paints was examined by Zieba–Palus [2]. Melamine and its salts are widely used in the formulation of fire retardant additive systems for polymeric materials [3, 4]. Melamine readily forms insoluble adducts with many organic and inorganic acids [5, 6]. Perchloric acid forms interesting complexes with organic cations. Both melamine and perchloric acid have got several industrial applications. Melamine molecule could be used as an organic part of investigated crystals. This molecule and its polymer found application in a wide variety of technological fields. Various studies on the adduct of melamine with urea, formaldehyde, and boric acid have been reported. [7, 8] The crystal structure of melaminium perchlorate monohydrate (MPM) was already reported by Zhao and Shi [9]. The title crystal is composed of melaminium cations, $C_3H_7N_6^+$, perchlorate anions ClO_4^-, and water molecules. Several researchers have already studied

N. Kanagathara
Department of Physics, Vel Tech Multi Tech Dr. Rangarajan Dr. Sakunthala Engg. College, Avadi, Chennai 600062, India

M. K. Marchewka
Institute of Low Temperature and Structure Research, Polish Academy of Sciences, P.O. Box 937, 50-950 Wrocław 2, Poland

N. Sivakumar · K. Gayathri · G. Anbalagan (✉)
Department of Physics, Presidency College, Chennai 600005, India
e-mail: anbu24663@yahoo.co.in

N. G. Renganathan
Department of Chemistry, Vel Tech Dr. RR Dr. SR Technical University, Avadi, Chennai 600062, India

S. Gunasekaran
PG & Research Department of Physics, Pachaiyappa's College, Chennai 600030, India

the thermal behavior of melamine [10–12]. Phase transformation of melamine at high pressure and temperature was studied by Yu et al. [13]. Nagaishi et al. [14] studied the thermal decomposition of the addition compound of melamine with hydrogen peroxide. Thermal and flame retardation properties of melamine phosphate-modified epoxy resins were studied by Chen et al. [15]. The presence of triazine ring in their structure gives improved hydrolytic and thermal stability [16]. TG is used to determine the thermal decomposition kinetics and thermal stability of polymers. This can be done by either single heating rate program like Coats–Redfern, Freeman–Caroll, Chang, or multiple heating rate programs like Friedmann, Flynn–Wall, Kissinger, and Kim–Park [17]. According to ICTAC kinetics committee, multiple heating rate programs is recommended. Since this method results only fewer errors than single heating rate method, to estimate kinetic parameters for the thermal decomposition of polymer composites, multiple heating rate method is applied. Although many reports available for the thermal behavior of melamine and its salts, not much research has been carried out on the kinetic analysis of the thermal decomposition of MPM. Hence, in this study, we report the growth of MPM single crystal. The grown crystal is characterized by using XRD, thermal stability has been done by thermogravimetric analysis. Thermal behavior of kinetics has been carried out and the results are discussed in detail in this communication. Dielectric studies have also been done to characterize dielectric behavior of the title crystal.

Materials and methods

Single crystals of MPM ($C_3H_7N_6^+ClO_4^-\cdot H_2O$) were grown by slow evaporation method. This growth was accomplished by mixing AR grade samples of melamine and perchloric acid in an appropriate ratio and stirred well, filtered and then allowed to cool. Tiny transparent and colorless crystals of the title compound were obtained after 3–4 weeks duration.

The grown crystals have been characterized by X-ray powder diffraction technique using Rich Seifert X-ray powder diffractometer with Cu Kα radiation of $\lambda = 1.5406$ Å in the 2θ range of 10°–70° by employing the reflection mode for scanning. The detector used was a scintillation counter. The sample was scanned at a rate of 1° min^{-1}. The thermal behavior of MPM was studied at 5, 10, and 20 °C min^{-1} by using a SDT Q 6000 V 8.2 Built 100 thermal analyzer. All the experiments were non-isothermal and were carried out under nitrogen atmosphere in the temperature range of 30–1,000 °C. Also the title crystal was subjected to dielectric studies using a HIOKI model 3532-50 LCR HITESTER with a conventional two terminal sample holder. The sample was electroded on either side with air-dying silver paste so that it behaves like parallel capacitor. The studies were carried out in the frequency range of 50 Hz–5 MHz and within the temperature ranging from 313 to 373 K.

Results and discussion

X-ray powder diffraction analysis

Figure 1 shows the indexed X-ray powder diffraction pattern for the grown title crystal. From the study, it is confirmed that the title crystal crystallizes in triclinic system (P-1) with the lattice parameters $a = 5.6275 \pm 0.0780$ Å, $b = 7.6926 \pm 0.1025$ Å, $c = 12.0878 \pm 0.2756$ Å, $\alpha = 103.89 \pm 1.01°$, $\beta = 94.61 \pm 0.92°$, $\gamma = 110.22 \pm 0.81°$, and $V = 468.95$ $Å^3$ and these values agree very well with the earlier literature [9]. The prominent peaks have been indexed. The sharp and well-defined Bragg's peaks at specific 2θ angles confirm the crystalline nature and purity of the title crystal.

Thermal studies

Thermogravimetric analysis is a powerful tool to characterize the variety of products in industry [18, 19]. TG–DTA curves of MPM at three different heating rates 5, 10, and 20 °C min^{-1} in the temperature range of 30–1,000 °C are shown in Fig. 2. It is seen from Fig. 2 that the decomposition of MPM occurs in three stages involving dehydration and decomposition. In the first stage, which takes place below ±120 °C suggesting that hydrated water of MPM is eliminated from the structure of the title compound and the corresponding exothermic DTA peak is obtained at

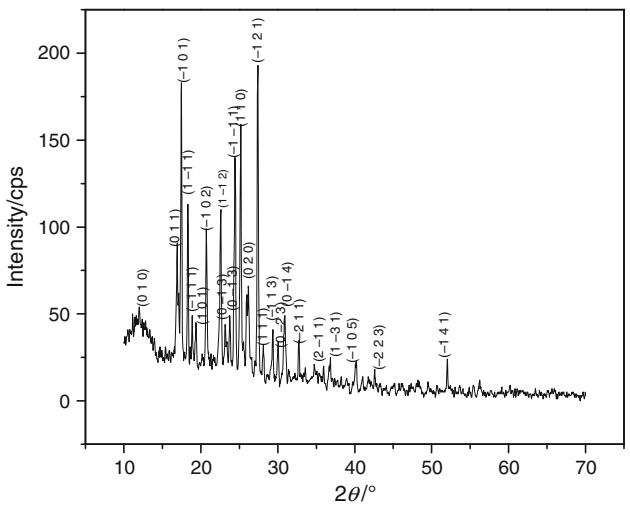

Fig. 1 Powder X-ray diffraction pattern of MPM

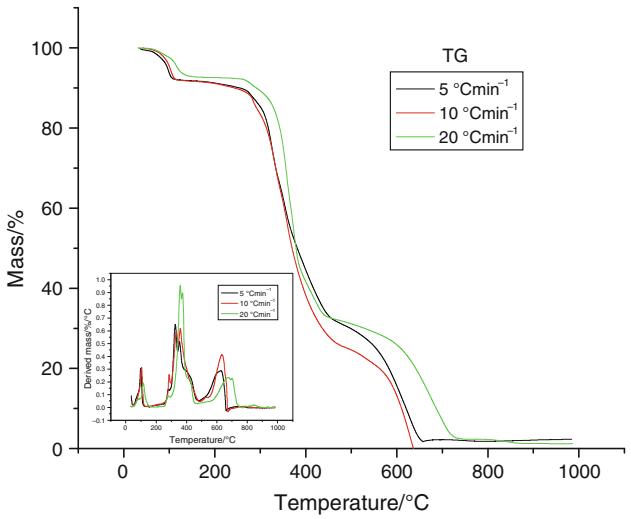

Fig. 2 TG–DTA curves of MPM in nitrogen atmosphere; heating rate of 5, 10, and 20 °C min^{-1}

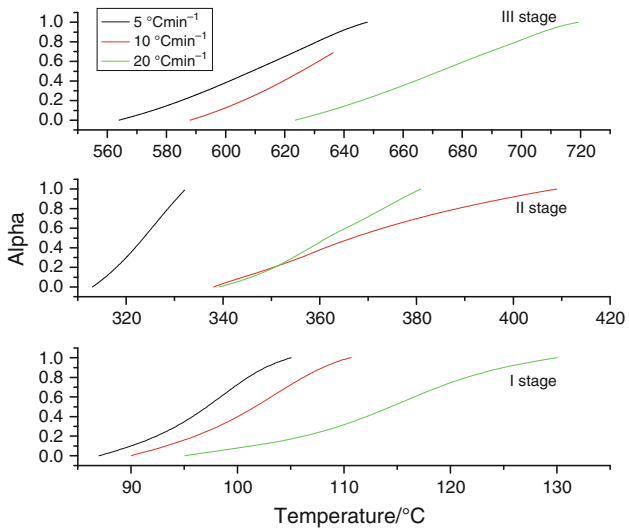

Fig. 3 Fraction reacted, α versus temperature for stages I, II, and III at three different heating rates

±110 °C. A rapid mass loss of nearly ±57 % occurs during the second stage which is due to the elimination of melaminium cations. This stage is attributed by three exothermic peaks which may be due to the decomposition of melamine. Generally, the thermal decomposition of melamine proceeds in stages and is accompanied by the detachment of ammonia. Melamine first decomposes into melam and then melon. The NH_2 groups in melam can be replaced by other atoms and groups [20]. Melaminium picrate [21] decomposes at 268 °C without any melting. But in the present case, melting occurs before decomposition. This is clearly seen in DTA curves (Fig. 2), i.e, a small hump appears before decomposition of melaminium cations. The remaining mass loss is accompanied by elimination of perchlorate anions in the third stage.

The TG curves shifted to higher temperatures as the heating rate is increased which is depicted in Fig. 2. This shows that definite heating rate has influence on the thermal decomposition [22].

TG kinetics method of thermal degradation

Large number of mathematical models has been proposed and used for studying kinetics and mechanism of such reactions using the TG data. Multiple heating rate data have been recommended for non-isothermal studies [23, 24]. Here, we studied the kinetics of the thermal decomposition of MPM at three different heating rates by three different multiple heating methods: Flynn–Wall, Kissinger, and Kim–Park [25–27].

The rate of degradation $\frac{d\alpha}{dt}$ can be expressed as the product of the function of temperature and the function of conversion: Typical graphs depicting fraction reacted, α versus temperature for three stages are shown in Fig. 3.

Flynn–Wall plots for three different heating rates against the temperature for the stages I, II, and III are shown in Figs. 4, 5, and 6, respectively, and the straight lines obtained are nearly to parallel to each other. At each heating rate, the temperatures were determined corresponding to extents of overall conversion 0.05–0.65 in intervals of 0.05. Activation energy (E_a) is calculated from the slope of the plot ln β versus $1/T$ for a fixed mass loss and it is given in Table 1. Activation energies calculated from the Kissinger and Kim–Park method are given in Table 2. The activation energy obtained for the three stages were found to be comparable with the result of Kissinger and Kim–Park method.

Figure 7a shows the relationship between the conversion (α) and effective activation energy (E_a). Effective

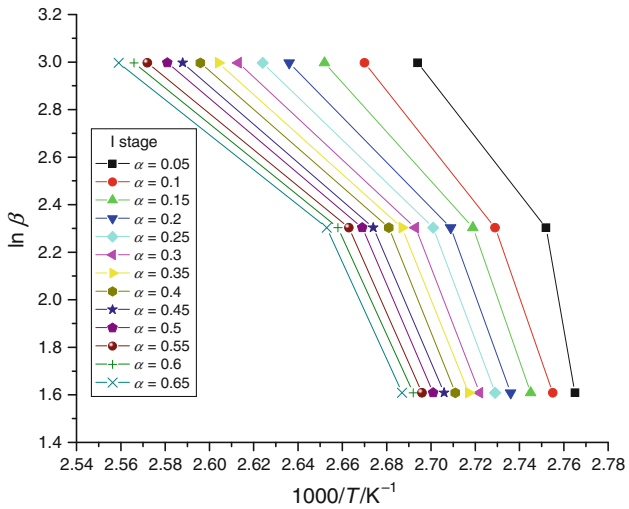

Fig. 4 Flynn–Wall plot for stage I in nitrogen atmosphere for the non-isothermal decomposition of MPM using TG data

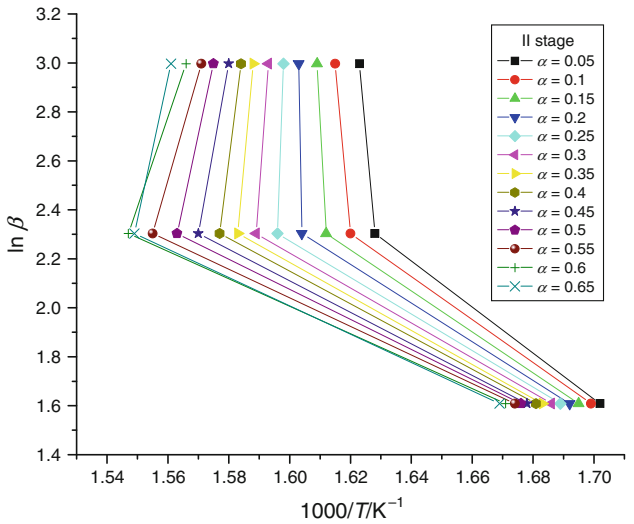

Fig. 5 Flynn–Wall plot for stage II in nitrogen atmosphere for the non-isothermal decomposition of MPM using TG data

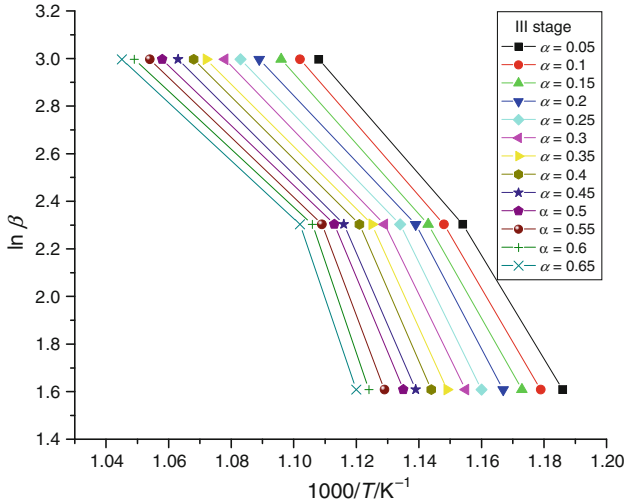

Fig. 6 Flynn–Wall plot for stage III in nitrogen atmosphere for the non-isothermal decomposition of MPM using TG data

activation energy can vary strongly with the temperature and the extent of conversion [28, 29]. If effective activation energy (E_a) is roughly constant over the entire conversion range, then it is said to be dominated by a single-step mechanism. In the present case, a significant variation in effective activation energy (E_a) with conversion (α) indicates that the process is kinetically complex, i.e., multi-step reaction mechanism [30]. E_a decreases with the extent of conversion (α) for the stages I and II except at $\alpha = 0.65$ for the stage II which is due to the exothermic decomposition of MPM. Effective activation energy is found to be very high for the stage III which indicates the significant variation with conversion. Dependence of effective activation energy (E_a) with extent of conversion (α) is used to identify its kinetic scheme, i.e., these values are used for input to multi-step for model fitting purposes [31]. Kinetic compensation effect was observed in many isothermal processes. The value of E_a bears a linear relationship with ln A viz

$$\ln A = aE + b, \tag{1}$$

where a and b are called compensation parameters. The compensation effect is valid for the thermal decomposition of MPM and it is shown in Fig. 7b.

Several researchers [31–35] reported the kinetic analysis by model fitting methods and dissociation mechanisms. Analysis of kinetics using different mechanisms based on kinetic models involve the selection of a "best fit" model which in turn depends on the value of statistical parameter r. In this study, the results are discussed only for the model which correlation is nearly 0.9–0.99.

A plot of ln $g(\alpha)/T^2$ versus 1,000/T shown in Fig. 8 for the stages I, II, and III almost give a straight line. For all the three stages, Avrami–Erofe'ev model is accepted [36]. The $g(\alpha)$ function can take the value of $-\ln(1-\alpha)^{1/2}$. Straight line with high correlation coefficient and low standard deviation values are selected to represent the possible controlling mechanism.

Dielectric studies

The dielectric properties are associated with the electro-optic property of materials; particularly, when they are non conducting materials [37]. The dielectric constant and dielectric loss are calculated using the equation $\varepsilon_r = Cd/\varepsilon_o A$, where A is the area of the sample and d is the thickness of the sample. The relative permittivity (ε_r) is usually known as permittivity. Figure 9 shows the temperature dependence of dielectric constant (ε_r) and dielectric loss (tan δ) for four different temperatures as a function of log frequency.

At low frequencies, all the four contributions may be active [38]. The high value of dielectric constant is attributed to high ionic conductivity. Most of the solid electrolytes have high dielectric constant. It is also observed that as the temperature increases, the value of dielectric constant also increases to a considerable value. The exchange of the charge carriers in the lattice sites is thermally activated by an increase in the temperature [39] resulting increase in dielectric constant. As the frequency increases, both the dielectric constant and dielectric loss values are found to decrease exponentially and attain constant values. The dielectric plot of the sample confirms the slight shift occurring with increase in frequency, which may be attributed to the excitation of electrons in the MPM single crystal lattice [40]. It is observed that the dielectric

Table 1 Kinetic parameters of non-isothermal decomposition of MPM by Flynn–Wall method

α	Flynn–Wall					
	Stage I		Stage II		Stage III	
	E_a/kJ mol^{-1}	ln A/s^{-1}	E_a/kJ mol^{-1}	ln A/s^{-1}	E_a/kJ mol^{-1}	ln A/s^{-1}
0.05	143.22	46.60	116.41	22.78	146.27	19.65
0.1	129.17	41.79	109.09	21.31	147.89	19.75
0.15	116.44	37.55	104.09	20.29	147.37	19.59
0.2	107.71	34.64	98.29	21.44	144.02	19.05
0.25	102.38	32.85	92.98	18.09	144.67	19.03
0.3	98.59	31.56	89.03	17.31	144.67	18.95
0.35	95.07	30.39	86.29	16.75	142.99	18.64
0.4	93.16	29.72	82.79	16.07	144.23	18.72
0.45	91.34	29.09	79.36	15.41	144.23	18.64
0.5	89.58	28.48	75.61	14.69	141.11	18.17
0.55	86.67	27.52	71.22	13.86	143.34	18.37
0.6	85.48	27.09	67.89	13.22	141.03	18.01
0.65	83.94	26.57	71.31	13.82	141.03	17.94

Table 2 Activation energies of thermal degradation of MPM by Kissinger and Kim–Park method

Method	Stage I		Stage II		Stage III	
	E_a/kJ mol^{-1}	ln A/s^{-1}	E_a/kJ mol^{-1}	ln A/s^{-1}	E_a/kJ mol^{-1}	ln A/s^{-1}
Kissinger	71.62	12.21	117.34	12.47	159.87	9.61
Kim–Park	77.94	27.09	127.59	27.32	175.24	25.26

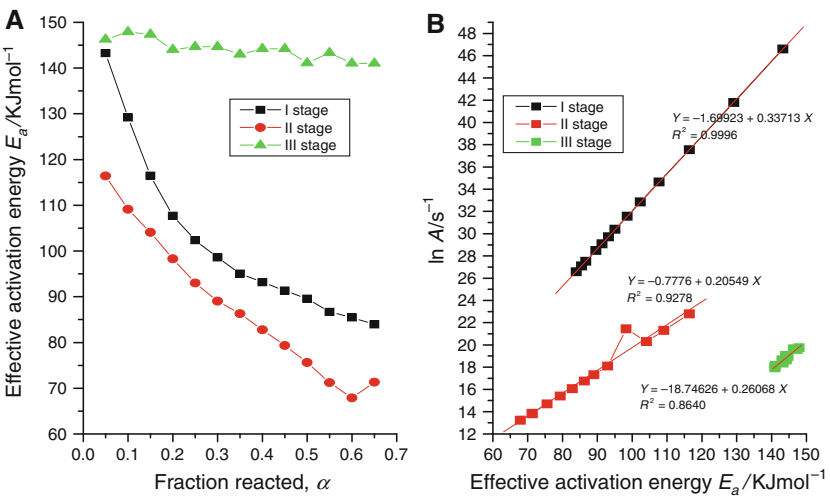

Fig. 7 **a** Variation of effective activation energy (E_a) versus fraction reacted (α) by Flynn–Wall method for three different stages I, II, and III; **b** plot of pre-exponential factor (ln A) versus effective activation energy (E_a)

loss decreases slowly with temperature for all frequencies and attains the steady value at high temperature. The increase in tan δ with temperature may be due to space charge polarization. The larger value of ε_r and tan δ at low frequency arises due to the presence of space charge polarization near the grain boundary interfaces which depends on the purity and perfection of the sample. At low frequencies, the dipoles can easily switch alignment with the changing field. As the frequency increases, the dipoles are less able to rotate and maintain phase with the applied field, thus they reduce their contribution to the polarization. The low dielectric loss at higher frequency of the sample indicates that title crystals posses lesser number of electrically active defects [38], and this parameter is of vital

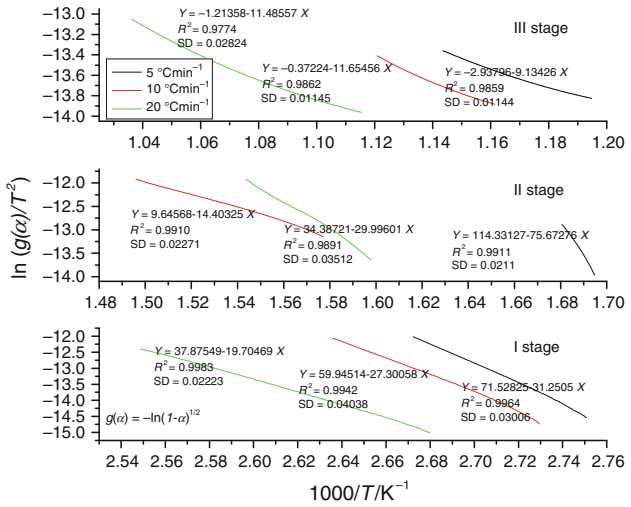

Fig. 8 Plot of $\ln[g(\alpha)/T^2]$ versus 1,000/T for stages I, II, and III using TG data

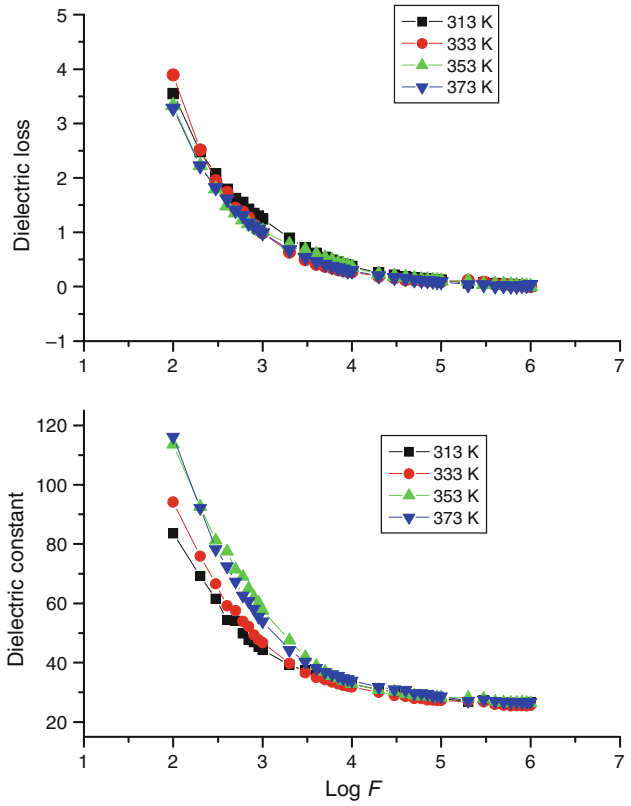

Fig. 9 Temperature dependence of dielectric constant (ε_r) and dielectric loss (tan δ) as a function of log frequency

importance for nonlinear optical materials in their application.

The variation in resistivity and conductivity with the frequency for the title crystal is shown in Fig. 10. The AC resistivity and AC conductivity were calculated using the relation

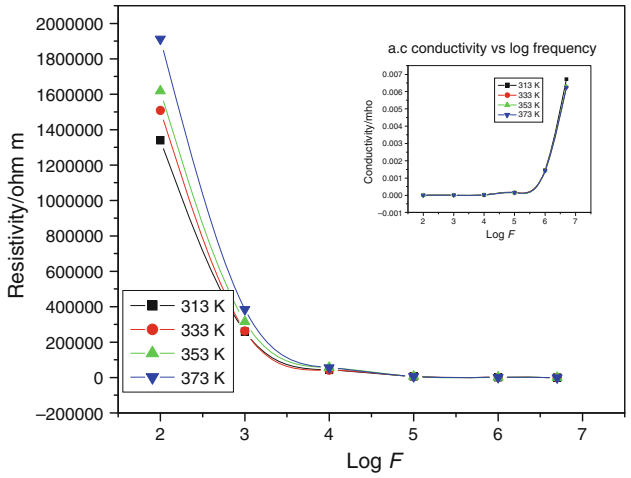

Fig. 10 AC resistivity and AC conductivity versus log frequency

$$\rho = A/2\pi fCd \quad \text{and} \quad \sigma_\rho = 1/\rho, \tag{2}$$

where C is the capacitance, d is the thickness, A is the area of the crystal, and f is the frequency of the applied field.

It is observed that the AC resistivity decreased rapidly as frequency increased. Obviously reverse trend was observed for AC conductivity of the grown crystals which is considered to be a normal dielectric behavior. Hence, conductivity increases with increases in temperature is due to the temperature dependence of the proton transport [41].

Conclusions

Single crystals of MPM have been grown by slow evaporation method. The grown crystals have been characterized by X-ray powder diffraction and it is found that it crystallizes in the space group P-1 with triclinic geometry. TG–DTA measurements were carried out at three different heating rates 5, 10, and 20 °C min^{-1}. Multiple heating rate methods: Flynn–Wall, Kissinger, and Kim–Park were used. The effective activation energies obtained by these methods are comparable. The plot of $1/T_p$ versus ln (β/T_p^2) for the stages showed a reasonable straight line with high correlation coefficiency. It is found that the activation energy obtained from Kim–Park method was higher than those from other methods. Dependence of effective activation energy with extent of conversion shows that the process is kinetically complex. The compensation effect is valid for thermal decomposition of MPM. From the dielectric study, it can be concluded that both dielectric constant and dielectric loss of the crystal decreases with increase in frequency attaining a constant value beyond 100 kHz. The low value of dielectric loss at high frequency suggests that the grown crystals possess good optical quality. This parameter is of vital importance for nonlinear optical materials in their applications.

Acknowledgements Author (M.K.M) acknowledges Ministry of Science and Higher Education (Grant No. NN507221840). One of the author (N.K) is highly thankful to Col. Vel R. Rangarajan, Chairman, Vel Group of Institutions, Chennai for the constant encouragement towards the research work and Dr. Jeya Rajendran, Department of Chemistry, Loyola College, Chennai for her fruitful suggestions.

References

1. Crews GM, Ripperger W, Kersebohm DB, Seeholzer J. Melamine and guanamines. Ullmann Encycl Ind Chem. 1990;16:171–85.
2. Zieba–Palus J. Application of micro-Fourier transform infrared spectroscopy to the examination of paint samples. J Mol Struct. 1999;511:327–35.
3. Kay M, Price AF, Lavery I. A review of intumescent materials, with emphasis on melamine formulations. J Fire Retard Chem. 1979;6:69–91.
4. Braodbent JRA, Hirschler MM. Red phosphorus as a flame retardant for a thermo plastic nitrogen-containing polymer. Eur Polym J. 1984;20:1087–93.
5. Bann B, Miller SA. Melamine and derivatives of melamine. Chem Rev. 1958;58:131–72.
6. Frazier AW, Gautney J, Cabier JL. Preparation and characterization of melamine sulfurous and sulfuric acid adducts. Ind Eng Chem Prod Res Dev. 1982;21:470–3.
7. Meier RJ, Maple JR, Hwang MJ, Hagler AT. Molecular modeling urea formaldehyde and melamine-formaldehyde resins—a force field for urea and melamine. J Phys Chem. 1995;99:5445–56.
8. Kawasaki T, Kuroda Y, Nishikawa H. Crystal structure of melamine diborate. J Ceram Soc Jpn. 1996;104:935–8.
9. Zhao MM, Shi PP. Melaminium perchlorate monohydrate. Acta Cryst. 2010;E66:o1463–70.
10. May H. Pyrolysis of melamine. J Appl Chem. 1959;9:340–4.
11. Van der Plaats G, Soons H, Snellings R. The thermal behavior of melamine. In: Proceedings of Second European symposium on thermal analysis. London: Heyden; 1981. p. 215–7.
12. Costa L, Camino G. Thermal behavior of melamine. J Therm Anal. 1988;34:423–9.
13. Yu DL, He JL, Liu ZY, Xu B, Li DC, Tioan MJ. Phase transformation of melamine at high pressure and temperature. J Mater Sci. 2008;43:689–95.
14. Nagaishi T, Matsumoto M, Yoshigana S. Thermal decomposition of addition compound of melamine with hydrogen peroxide. J Therm Anal. 1990;36:55–60.
15. Chen W-Y, Wang Y-Z, Chang F-E. Thermal and flame retardation properties of melamine phosphate-modified epoxy resins. J Polym Res. 2004;11:109–17.
16. Siimer K, Cristjanson P, Kaljuvee T, Pekh T, Lasn I, Saks I. TG–DTA study of melamine–urea–formaldehyde resins. J Therm Anal Calorim. 2008;92:19–27.
17. Li XG. Thermogravimetric kinetics of thermotropic copolyesters containing *p*-oxybenzoate unit by multiple heating-rate methods. J Appl Polym Sci. 1999;74:2016–28.
18. Gabott P. Principles and applications of thermal analysis. Oxford: Blackwell; 2008.
19. Brown ME. Handbook of thermal analysis and calorimetry, vol. 1. Amsterdam: Elservier; 2003.
20. Franklin EC. The ammono carbonic acids. J Am Chem Soc. 1922;44:486–509.
21. Seifer GB. Cyanuric acid and cyanurates. Russ J Coord Chem. 2002;28:301–24.
22. Shin SM, Kim SH. Thermal decomposition behavior and durability evaluation of thermaotropic liquid crystalline polymers. Macromol Res. 2009;17:149–55.
23. Vyazovkin S, Burnham AK, Craida JM, Perez-Maqueda LA, Popescu C, Sbirrazzuoli N. ICTAC kinetics committee recommendations for performing kinetic computations on thermal analysis data. Thermochim Acta. 2011;520:1–19.
24. Brown ME, Maciejewski M, Vyazovkin S, Nomen R, Sempere J, Burnham A, Opfermann J, Strey R, Anderson HL, Kemmler A, Keuleers R, Janssens J, Desseyn HO, Li CR, Tang TB, Roduit B, Malek J, Mitsuhashi T. Computational aspects of kinetic analysis Part A: the ICTAC kinetics project-data, methods and results. Thermochim Acta. 2000;355:125–43.
25. Vyazovkin S. Kinetic concepts of thermally stimulated reactions in solids, a view from a historical perspective. Int Rev Phys Chem. 2000;19:45–60.
26. Vyazovkin S. On the phenomenon of variable activation energy for condensed phase reactions. New J Chem. 2000;24:913–7.
27. Prout EG, Tompkins FC. Thermal decomposition of potassium permanganate. Trans Faraday Soc. 1944;40:488–98.
28. Rajendran J, Thanu Lingam L, Jose M, Jerome Das S. Kinetics and dissociation mechanism of heptaaqua-*p*-nitrophenolato strontium (II) nitrophenol. J Therm Anal Calorim. 2011;103:845–51.
29. Flynn JH, Wall LA. A quick, direct method for the determination of activation energy from thermogravimetric data. J Polym Sci B Polym Lett. 1966;4:323–8.
30. Kissinger HE. Reaction kinetics in differential thermal analysis. Anal Chem. 1957;27:1702–6.
31. Kim S, Park JK. Characterization of thermal reaction by peak temperature and height of DTG curves. Thermochim Acta. 1995;264:137–56.
32. Jankovit B, Mentus S, Jankovit M. A kinetic study of the thermal decomposition process of potassium metabisulfite: estimation of distributed reactivity model. J Phys Chem Solids. 2008;69:1923–33.
33. Vyazovkin S, Dranca I. Isoconversional analysis of combined melt and glass crystallization data. Macromol Chem Phys. 2006;207:20–5.
34. Alzina C, Sbirrazzuoli N, Mija A. Hybrid nanocomposites: advanced non linear method for calculating key kinetic parameters of complex cure kinetics. J Phys Chem B. 2010;114:12480–7.
35. Srivastava P, Kapoor IPS, Singh G. Thermolysis of pyridinium perchlorate salts. Indian J Eng Mater Sci. 2009;16:423–8.
36. Starink M. The determination of activation energy from linear heating rate experiments; a comparison of the accuracy of isoconversion methods. J Thermochim Acta. 2003;404:63–76.
37. Boomadevi S, Mittal HP, Dhansekaran R. Synthesis, crystal growth and characterization of 3-methyl 4-nitropyridine 1-oxide (POM) single crystals. J Cryst Growth. 2004;261:55–62.
38. Rao KV, Samakula A. Dielectric properties of cobalt oxide, nickel oxide and their mixed crystals. J Appl Phys. 1965;36:2031–8.
39. Balarew R, Duhlew R. Application of the hard and soft acids and bases concept to explain ligand coordination in double salt structures. J Solid State Chem. 1984;55:1–6.
40. Prabha K, Rajesh Kumar T, Du SF, Vimalan M, Dayalan A, Sagayaraj P. Growth and characterization of a new nonlinear optical barium strontium borate (BSB) single crystals. Mater Chem Phys. 2010;121:22–7.
41. Meena M, Mahadevan CK. Growth and electrical characterization of L-arginine added KDP and ADP single crystals. Cryst Res Technol. 2008;43:166–72.